Sveriges lantbruksuniversitet
Swedish University of Agricultural Sciences

Department of Soil and Environment

A novel platform to quantify crack formation due to root water uptake

Susanne Alexandersson

Master's Thesis in Soil Science
Agriculture Programme – Soil and Plant Sciences

Examensarbeten, Institutionen för mark och miljö, SLU
2019:02

Uppsala 2019

A novel platform to quantify crack formation due to root water uptake

En ny plattform för att kvantifiera sprickbildning till följd av rotvattenupptag

Susanne Alexandersson

Supervisor: Tino Colombi, Department of Soil and Environment, SLU
Assistant supervisor: Thomas Keller, Department of Soil and Environment, SLU
Examiner: Nicholas Jarvis, Department of Soil and Environment, SLU

Credits: 30 ECTS
Level: Second cycle, A2E
Course title: Master thesis in Soil science, A2E – Agriculture Programme – Soil/Plant
Course code: EX0881
Programme/Education: Agriculture Programme – Soil and Plant Sciences 270 credits (Agronomprogrammet – mark/växt 270 hp)
Course coordinating department: Soil and Environment

Place of publication: Uppsala
Year of publication: 2019
Title of series: Examensarbeten, Institutionen för mark och miljö, SLU
Number of part of series: 2019:02
Online publication: http://stud.epsilon.slu.se

Keywords: soil structure dynamics, root water uptake, crack formation, automatized imaging system

Sveriges lantbruksuniversitet
Swedish University of Agricultural Sciences

Faculty of Natural Resources and Agricultural Sciences
Department of Soil and Environment

Abstract

Soil structure play an important role for a productive and sustainable agriculture. It controls many processes in the soil and has a great impact on soil functions and related ecosystem services. Plants play an important role in soil structure dynamics. The soil structure changes due to plant water uptake, but the overall influence is still far from being fully understood. Both spatial and temporal quantifications of these dynamics are missing, partly because lack of appropriate methods.

The aims of the study were (i) to develop an experimental set-up that allows the study of crack formation around roots due to root water uptake at high spatial (10 µm) and temporal (2 min) resolution using automated RGB time-lapse imaging (ii) to conduct and evaluate the methodological approach. The experiment was carried out in a module-based imaging platform, which consists of a framework, cuvettes including inserted roots and soil, a drying system and an imaging system. This study tested the set-up (i.e. proof of concept) under different scenarios including two different soil types (clay and loam) and two levels of root water potentials (-350 kPa and -1500 kPa). The employed experimental method provided images every second minute over a time period of seven days. The experiment resulted in images with a quality to make visual assessments and quantifications of the emerging cracks.

The results showed that plant water uptake affects crack formation differently depending on soil type and root water potential. Soils with higher clay content and/or a lower root water potential induce more and relatively longer and wider cracks. This is expected as clay contains expansive properties of the soil and a lower root water potential dries the soil to a greater extent. Overall, the results demonstrate that the employed method is both useful and valid to study crack formation due to plant water uptake. It has the capacity to provide images with a quality to make visual assessments of crack formation and quantification of the spatial configuration of emerging cracks.

Keywords: Soil structure dynamics, root water uptake, crack formation, automatized imaging system

Sammanfattning

Markstrukturen har stor betydelse för ett produktivt och hållbart jordbruk. Den kontrollerar många processer i marken och har stor inverkan på markens funktioner och relaterade ekosystemtjänster. Växter påverkar markstrukturen genom rötternas vattenupptag som orsakar sprickbildning. Det finns fortfarande kunskapsluckor över vattenupptagets fulla effekt på sprickbildning. Både spatiala och temporala kvantifieringar av denna dynamik saknas, vilket bland annat beror på att det saknas lämpliga metoder för att studera detta.

Syftet med denna studie var (i) att utveckla en metod som möjliggör att studera sprickbildning runt om rötter till följd av rotvattenupptag vid hög spatial (10 µm) och temporal (2 min) upplösning, samt (ii) testa och utvärdera metoden. Experimentet genomfördes i en modulbaserad bildplattform, som består av en ramkonstruktion, kyvetter med artificiella rötter och jord, ett torkningssystem samt ett bildtagningssystem.

Metoden testas under olika scenarier, som inkluderade två jordtyper med olika lerhalt och två nivåer av rotvattenpotentialer (-350kPa och 1500kPa). Metoden genererar bilder på kyvetterna varannan sekund över en tidsperiod på sju dagar. Bilder har tillräcklig hög kvalitét för att göra visuella bedömningar av sprickbildning men skapar även förutsättningar för kvantifiering av den spatiala konfigurationen av framträdande sprickor.

Resultaten visade att växternas vattenupptag påverkar sprickbildningen och torkningen av jorden olika beroende av jordtyp och rotvattenpotential. En jord med högre lerhalt och/eller lägre rotvattenpotential inducerar fler och relativt större, i termer av längre och bredare, sprickor. Detta är förväntat eftersom lerpartiklar utgör de expansiva egenskaperna hos en jord samt att den lägre rotvattenpotentialen torkar ut jorden i en högre utsträckning. Sammantaget visar resultaten att den som används i denna studie är både användbar och tillförlitlig för att studera sprickbildning till följd av rotvattenupptag.

Nyckelord: Markstruktur dynamik, rotvattenupptag, sprickbildning, automatiserad bildtagning

Populärvetenskaplig sammanfattning

Markstruktur definieras av hur markens mineralpariklar (oorganiskt material), organiska material och porer är rumsligt fördelade och förhåller sig till varandra. Markstrukturen påverkar många processer i marken och har stor inverkan på markens funktioner och relaterade ekosystemtjänster. En god markstruktur är viktigt för ett produktivt och hållbart jordbruk.

Det finns många faktorer som påverkar markstrukturen, såväl naturliga som mänskliga faktorer. En naturlig faktor är växter. Växter är viktiga för markstrukturdynamiken, exempelvis genom rötternas vattenupptag. När rötter tar upp vatten leder det till att jorden torkar upp runt omkring och krymper. Detta kan resultera i sprickbildning.

Många tidigare studier har undersökt relationen mellan rotvattenupptag och markens egenskaper. Samtidigt saknas det fortfarande kunskap om rotvattenupptagets effekt på sprickbildning. En orsak till detta är att det saknas lämpliga metoder. För att bättre förstå den fulla effekten som vattenupptag från rötter har på sprickbildningen behövs adekvata metoder som möjliggör kvantifiering av den rumsliga (spatiala) och tidsmässiga (temporala) utvecklingen av sprickor.

Syftet med denna studie var (i) att utveckla en metod som möjliggör att studera sprickbildning runt om rötter till följd av rotvattenupptag vid hög spatial (10 µm) och temporal (2 min) upplösning, samt (ii) testa och utvärdera metoden. Experimentet genomfördes i en modulbaserad bildplattform som består av en ramkonstruktion; kyvetter med artificiella rötter och jord; ett torkningssystem: polyetylenglukol (PEG) lösning och pumpar; samt ett bildtagningssystem. Metoden testades under olika scenarier där vi använde oss av två jordar med olika lerinnehåll och två olika nivåer av rotvattenpotential.

Huvudkonceptet var att simulera rotvattenupptag och undersöka effekten på sprickbildningen i jordarna. För att simulera rotvattenupptag lät vi en PEG-lösning (PEG är ett substrat som möjliggör att erhålla en lösning med specifik osmotisk potential) pumpas runt genom artificiella rötterna (halvgenomträngligt membran) som var placerade i jordfyllda kyvetter. Den skillnad i

vattenpotential som uppstod mellan vattnet i jordarna och rotvattenpotentialen (dvs potentialen i PEG-lösningen), resulterade i att vattnet i jorden sögs upp av rötterna och jordarna torkades ut, varpå sprickor bildades.

För att erhålla information och kunna studera uppkomna sprickor togs bilder med regelbundna tidsintervaller (2 minuter) i hög rumslig upplösning (<20 μm) under en period på sju dagar. Både kamerornas rörelser och bildtagning var automatiserad.

Med hjälp av högupplösta bilder kunde vi studera hur sprickbildning i jordarna utvecklats. Den kvantitativa bedömningen fokuserade på antalet sprickor samt längd och bredd. Vi undersökte även på hur jorden runt roten hade torkat efter att experimentet var avslutat. För denna analys beräknades medelförändringen av vatteninnehållet som sedan visualiserades i diagram med hjälp av statistiksystemet R.

Resultaten visade att växternas vattenupptag påverkar sprickbildningen olika beroende av jordtyp och rotvattenpotential. Sprickorna blir flera och tenderar att bli längre och bredare om jorden innehåller mera lera. Detsamma gäller om rotvattenpotentialen är lägre. Detta är förväntat eftersom lerpartiklar utgör de expansiva egenskaperna hos en jord samt att den lägre rotvattenpotentialen torkar ut jorden i en högre utsträckning. Sammantaget visar resultaten att metoden är både användbar och tillförlitlig för att studera sprickbildning till följd av rotvattenupptag. Metoden kan alltså användas för att generera fler resultat om sprickbildning i framtida studier.

I ett planerat experiment kommer denna metod användas tillsammans med ett automatiserat protokoll i syfte att förbättra bildanalysen. Tanken är att detta protokoll ska göra det möjligt att resultera i kvantitativa data innehållande mycket detaljerad information om sprickornas utveckling. Denna information ska kunna nyttjas för att analysera exempelvis sprickors totala area, antalet sprickor på en yta, sprickornas längd samt bredd. Denna kunskap skulle kunna bidra till en mera komplett förståelse för de processer och interaktioner som reglerar formationen av markstrukturen. Förhoppningen är att detta ska ge värdefull kunskap om markens egenskaper som i sin tur är viktig för en utveckling mot ett hållbart jordbruk.

Table of contents

1 Introduction

Soil is a living system and its structure, i.e. its geometrical arrangement of mineral and organic particles and the resulting pore space, is important for a productive and sustainable agriculture. Soil structure controls many processes in the soil and is central to most soil functions and ecosystems services. It directly impacts air permeability, hydraulic conductivity and biological activity, and influence fluxes and storage of water, gas and nutrients and mechanical properties (Vereecken et al. 2016, Rabot et al. 2018). Soil structure is also vital to biomass production as it influence the ability of root penetration that affects root distribution, which in turn, affects the capacity of water uptake and nutrient acquisition (Bronick & Lal 2005). Soil structure is influenced by numerous natural and anthropogenic factors and processes including clay content and type, climate, plants and biological features and human interventions. This implies that soil structure evolves over time and is thus a dynamic rather than a static scaffold (Angers & Caron 1998, Guimarães et al. 2017). Hence, it is not surprising that there is a rich body of literature on the topic of soil structure and soil structure dynamics due to its vitality and complexity (e.g. Young 1998, Angers & Caron 1998, Bodner et al. 2013, Rabot et al. 2018).

Plants influence soil structure dynamics through root penetration, root exudates, dead root decomposition, root entanglement and changed water regime (Six et al. 2004). Water uptake by the plant roots dries the soil. The water reduction causes shrinkage of the soil and formation of cracks (Oades 1993, Guimarães et al. 2017). However, the impact of root water uptake on soil shrinkage and crack properties (length, width, density and number) strongly depends on the clay content and the rate of which water is extracted, which in turn, depends on the root water potential. Although many studies have examined root water uptake and soil properties relations (e.g. Garrigues et al. 2006, Daly et al. 2018), crack formation due to plant water uptake is still not fully understood. For instance, there are still gaps in the knowledge regarding the spatial and temporal quantifications of crack development due to root water uptake. To understand and explain this,

suitable methods are needed. To date, there are no appropriate methods that enable quantification of these dynamics at high spatiotemporal resolution. Developing adequate methods is necessary to enhance a mechanistic understanding regarding the relationships between plant water uptake and soil structure dynamics. In general, such knowledge would contribute to providing a more complete picture of the processes and interactions that regulate soil structure formation.

Approaches based on imaging techniques have enabled researchers to examine a range features and processes in soil structure dynamics. More specifically, X-ray computed tomography (CT), neutron radiography, magnetic resonance imaging (MRI) and light transmission imaging (Carminati et al. 2016, Vereecken et al. 2016, Wang et al. 2018) have enabled non-destructive images and rapid visualisations of the soil and root environment at a range of different resolutions (Helliwell et al. 2017). However, although these are useful techniques they are restricted to relatively low spatiotemporal resolution. In an attempt to explain soil structure dynamics with a focus on cracking dynamics and formation due to water reduction, DeCarlo & Shokri (2014) examined the effect of a coarse-textured substrate on the cracking dynamics and morphology of an overlying kaolinite clay layer. Evaporating surfaces were recorded using an automatic imaging system, revealing properties of emerging cracks. Although there have been several important technical advancements in related research, there seems to be no detailed examinations and quantifications of crack formation due to plant water uptake at high spatiotemporal resolution.

The aim of this study was twofold. The first aim was to develop an experimental set-up that enables quantification of crack formation and the drying of soil around roots due to root water uptake at high spatial (10 µm) and temporal (2 min) resolution using automated RGB time-lapse imaging. The second aim was to evaluate the methodological approach. The employed method was tested in an experimental case study under different scenarios, i.e. two different soils and two levels of simulated root water potentials. The hypothesis was that the effect on crack development and drying of the soil is larger with a higher clay content and with a lower root water potential.

The study is organized as follows. Chapter 2 provides a background to soil structure dynamics. Chapter 3 describes the materials and the method. Chapter 4 describes the experimental case study and Chapter 5 presents the main results. Chapter 6 discuss the main outcome from this study. Conclusions are found in Chapter 7.

2 Background

2.1 Soil structure definition

Soil consists of a solid phase and void space. The solid phase constitutes of mineral and organic particles. The space that is not occupied by the solid material are voids, i.e. soil pores. These pores contain water and gas in varying proportions. Dexter (1991) defines soil structure as the spatial arrangement of mineral and organic particles and associated pore space. Structural stability, resiliency and vulnerability are often added to this definition, because soil structure is not a static property but considerably dynamic, responding to internal and external stresses and processes and thereby varying both spatially and temporally (Kay 1998). Structural stability refers to the resistance of a particular arrangement to internal and external stresses (Oades 1993) and structural resiliency refers to the capacity of natural processes to promote the recovery of soil structural form or stability when an applied stress is removed. In addition, structural vulnerability reflects the combined characteristics of stability and resiliency (Angers & Caron 1998, Johannes 2016).

The solid phase and the pore space are complementary aspects of soil structure, which can be approached from both perspectives, based on what is actively being shaped: soil aggregates or soil pores (see Rabot et al. 2018 for further aspects on these two perspectives). Pores resulting from the arrangement of soil primary particles are called textural pores and pores resulting from biological activity, climatic forces and management practices are called structural pores (Rabot et al. 2018). Pores can be divided into hierarchical categories, depending on their size: micropores (0-0.2 um); mesopores (0.2-50 um) and macropores (> 50 um). According to Six et al. (2004), pores can also be divided into following hierarchical categories: (I) macropores; (II) pore space between macroaggregates; (III) pores between

microaggregates; and (IV) pores within microaggregates. Such classifications may help in the understanding of soil structure.

2.2 Soil structure controls soil processes and functions

Soil structure is important for a productive and sustainable agriculture. Its properties mediate many important key soil processes, from the pore/single root, micrometre to metre, to the landscape scale, and influences soil functions (Young et al. 1998). Important soil properties are bulk density, total porosity, air-filled porosity, air permeability and saturated hydraulic conductivity (Keller et al. 2017). Rabot et al. (2018) argue that soil structure controls many processes in soils, and regulates water retention and infiltration, gaseous exchanges, soil organic matter and nutrient dynamics, root penetration, and the susceptibility to erosion and compaction.

Soil structure impacts functions and ecosystem services such as biomass production (food, fiber, and fuel) and water provision. It also influences environmental quality in terms of water purification and atmospheric regulation, in particular soil carbon sequestration (Zhang et al. 2007, Vereecken et al. 2016). Furthermore, soil structure constitutes habitats for many soil organisms and is thus important for biodiversity and biological activity (Rabot et al. 2018). Since soil processes and functions impact water availability and oxygen supply for the plants, there is a strong link between soil structure and plant growth. Finally, the ability of roots to penetrate soil is crucial as the root distribution influences the capacity of water uptake and nutrient acquisition (Bronick & Lal 2005).

2.3 Soil structure dynamics

Soil structure evolves over time and is thus dynamic rather than a static scaffold. Factors influencing soil structure dynamics are anthropogenic and natural processes: abiotic and biotic processes.

2.3.1 Abiotic and biotic factors

Abiotic factors include inherent soil properties, i.e. clay content and type, and climate that results in wetting and drying, freezing and thawing (Angers & Caron 1998). The parent material determines the development of texture and soil constituents, i.e. phyllosilicates, sesquioxides, carbonates. Climate affects soil structure as it controls the freezing-thawing and wetting-drying cycles, which induce shrink and swell behaviour of the soil.

The result is reorientation of particles and crack development (Kay 1998, Johannes 2016). Some clay particles swell while binding water and shrink due to loss of water. The shrinkage and swelling behaviour of a given soil depends thus on the content of these clay minerals. The shrink and swell capacity is virtually zero in a sand soil, so drying and wetting cycles do not alter the structure significantly. In loam and clay soil, the shrink and swell capacity is greater. Soil with higher clay content undergoes greater changes. The higher clay content, the more powerful the cycles of structural formation during drying and wetting cycles (Oades 1993).

Important biotic factors include plants, microorganisms (bacteria and fungi), mesofauna (arthropods) and macrofauna (e.g. earthworms and moles) (Angers & Caron 1998). Plant roots affect the soil structure through plant water uptake and changed water regime, root penetration, root exudates, dead root decomposition and root entanglement (Six et al. 2004). While penetrating the soil, roots may enlarge existing biopores or create new ones by displacing soil particles. Roots and root exudates stabilize aggregates through anchorage and mucilage secreted from roots acting like biological glue. This glue-like substance binds the soil particles together. Furthermore, plant roots and litter contribute indirectly to macropore formation. This by serving as food for the fauna, in particular earthworms (Angers & Caron 1998, Jin et al. 2017).

Macro- and mesofauna are known as soil engineers, as they are central for the formation of soil pores. Through their activities, particles are displaced and biopores are created, which may have an effect on the porosity, the bulk density and the infiltration capacity of the soil (Elkins et al. 1986, Lavelle et al. 1997). Earthworms contribute not only to increased porosity by creating burrows, they also contribute to the stability of aggregates. They produce casts that constitute more stable aggregates than the bulk soil (Jangorzo 2015). Furthermore, microorganisms contribute to the stabilisation of soil structure. Fungi mycelium entangles particles within the hyphae network and cements particles together through extracellular polysaccharide production. The production of mucilages by bacteria and fungi contribute to the stabilisation of microaggregates (Tisdall et al. 1997, Six et al. 2004).

When comparing how biotic and abiotic factors influence soil structure, it may be important to consider sandy soils, loams and clay soils separately. This because expansive properties of soils are controlled by clay particles (Oades 1993). Furthermore, one should distinguish between single particle structure and aggregate structure. In a single particle structure, pure sand for instance, the particles do not adhere to each other to any great extent.

The primary particles are relatively large and the cohesion between them is weak. A soil that consists of colloids, i.e. clay minerals and humus particles, may result in aggregates with compounded primary particles (Eriksson et al. 2011). Thus, the effect on soil structure in sandy soil depends more on biotic factors rather than abiotic factors. In a clayey soil, on the other hand, the influence on soil structure depends on both abiotic and biotic factors.

2.3.2 Anthropogenic factors

Anthropogenic processes are primarily human interventions, such as soil tillage, vehicle traffic, incorporation of organic fertilizers and amendments, but also crop selection and fertilization (Guimarães et al. 2017). Modern heavy machinery may induce stresses in the soil that exceed the mechanical strength in the soil, which results in soil deformation and altered soil structure (Keller et al. 2017). The use of heavy machinery can decrease soil porosity and increase bulk density. Soil cultivation influences the carbon balance in soil, partly by removing more soil organic carbon (SOC) than carbon inputs. Furthermore, soil tillage loosens and fragments the soil and modifies the soil structure. It also influences the biological activity and enhance the carbon mineralisation (Johannes 2016).

2.4 Plant water uptake

Plant water uptake is fundamental since water are essential for plant growth. Differences in water potential between the bulk soil and the rhizosphere, i.e. the soil in contact and influenced by roots, result in water flow from the bulk soil towards the root surface. A gradient in water potential across the tissue of the root enables water to flow into the root. This gradient depends upon the flow rate and the hydraulic conductivity of the root (Carminati et al. 2010, 2016).

Factors influencing water uptake by the root are root density, soil hydraulic functions, root mucilage, soil water status and suction of the root (Vereecken et al. 2016). York et al. (2016) explains that water depletion zones are expected to form around the roots when the hydraulic conductivity of soil is not large enough to sustain root water uptake. A decreasing water content towards the roots implies that the gradient in soil water potential drives water to the root surface. The lesser the soil hydraulic conductivity, the greater the potential gradients needed to sustain root water uptake. Water uptake by the plant roots dries the soil. The effect of this water reduction is shrinkage of the soil and formation of cracks (Oades

1993, Guimarães et al. 2017).

To what extent the soil shrinks when drying and swells when rewetting, and thus affects crack development, depends strongly on the mineralogy and the clay content. As for the drying and wetting cycles, the higher the clay content the more vigorous the cycles of structural formation (Oades 1993). Soil shrinkage also depends on the rate of which water is extracted. The impact on crack properties, such as crack length, crack width, crack density and crack numbers, strongly depends on the clay content and the rate of root water uptake, which, in turn, is partially controlled by the root water potential, which may differ greatly (Ball & Oosterhuis 2005).

2.5 Approaches to study soil structure dynamics

Several studies have examined soil structure dynamics (Tracy et al. 2012, Starkloff et al. 2017, Wang et al. 2018). A range of methods have been developed and used in this endeavour. In particular, imaging techniques have enabled research to be explicit about features and processes in soil structure dynamics. Contemporary techniques include X-ray computed tomography (CT), neutron radiography, magnetic resonance imaging (MRI) and light transmission imaging (Carminati et al. 2016, Vereecken et al. 2016). These approaches have enabled non-destructive images and rapid visualisations of the soil and root environment, and a better understand of the failure mechanisms (Helliwell et al. 2017). Taina et al. (2008) argue that CT can be used to quantify soil structure. Three-dimensional (3D) X-ray CT can make non-destructively analyses of the internal spatial structure of samples. Wang et al. (2018) used this technique to analyse spatial structural dynamics in clay due to freezing-thawing cycles. Similarly, Starkoff et al. (2017) employed X-ray CT to quantify the effects of freezing-thawing cycles on pore network of a silt and a sandy soil. Their study shows that freezing-thawing affected the looser sandy soil more than the silt with its more cohesive structure.

Electrical resistivity tomography (ERT) is another technique to study non-destructive and continuous characterization of, for instance, desiccation cracks and induced heterogeneities in soil. Keller et al. (2017) made use of ERT to investigate changes in soil physical properties. Relative changes in inferred electrical resistivity between the time before and after compaction were measured to investigate effect of soil compaction. In a recent study, Tang et al. (2018) used ERT in combination with image processing to examine the development of desiccation cracks and quantify geometrical characteristics of surface crack patterns. Although this is a useful technique

to investigate different aspects of soil structure dynamics, they are restricted to relatively low spatiotemporal resolution.

A recent contribution based on 2D techniques, such as DeCarlo & Shokri (2014), have sought to improve this. They examined the effect of a coarse-textured substrate on the cracking dynamics and morphology of an overlying kaolinite clay layer. The aim was to understand cracking dynamics and formation. To do this, they used an automatic imaging system to record samples at the evaporating surface in five-second intervals with 140µm/pixel resolution. In the post image segmentation, the images were compared to a reference image taken in the beginning of the experiment. One of the conclusions was that the extent of cracks, characterized by cracking length and density, decreased with increased substrate particle size. A variable and wider crack width distribution was also observed.

3 Materials & Method

3.1 Main concept

The main concept is to simulate root water uptake and examine how this affects crack development in soils. To simulate root water uptake, polyethylene glycol (PEG)-solution is pumped through artificial roots (semipermeable tubes) allocated inside soil-filled cuvettes. The generated water potential gradient between the soil water potential in the cuvettes and the root water potential, i.e. the PEG-solution, results in drying of the soils in the cuvettes. Figure 3.1 is a conceptual drawing of the pumping system and shows how the solution flows from the PEG-reservoir, through the cuvettes and back to the PEG-reservoir. To record emerging cracks, images are made in regular time intervals (2 minutes) at high spatial resolution (< 20 µm) using the cameras dolly system.

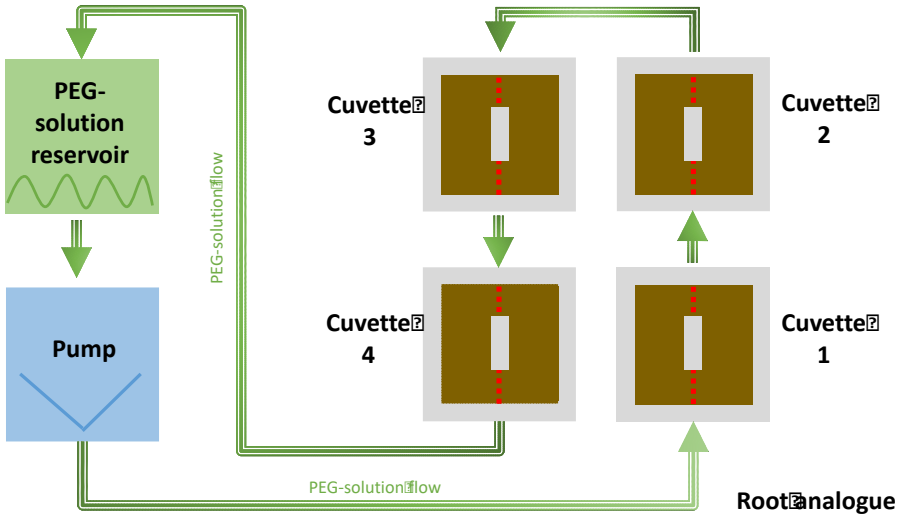

Figure 3.1. Conceptual drawing of the pumping system, the arrows show how the solution flows from the PEG-reservoir, through the pumps and the cuvettes and thereafter back to the PEG-solution reservoir

3.2 Platform design

The module based imaging platform consists of an aluminium frame; soil cuvettes and artificial roots; drying system: polyethylene glycol (PEG) solution and pumps; and a time-lapse imaging system. Figure 3.2 provides an overview of the platform, illustrating the aluminium frame with the cuvettes and the time-lapse imaging system.

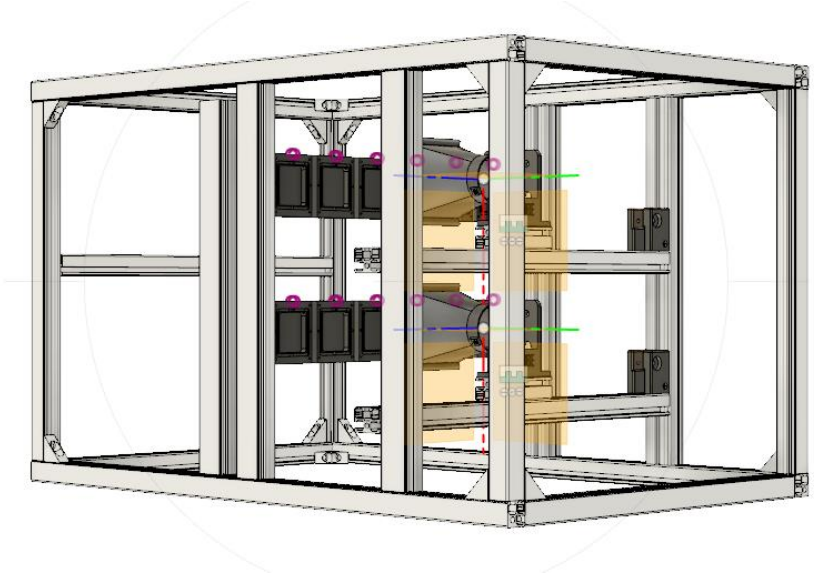

Figure 3.2. The figure illustrates the aluminium frame including the soil cuvettes and the time-lapse imaging system

3.3 Aluminium frame

The frame is made of aluminium profiles 31.5 X 31.5 (N 0163) and 31.5 X 45 (N 0164). The different parts are connected by standard M8 screw fixings. The bases of the sleds are also made of profiles connected with a smooth guide (N 1363) manufactured by Norcan Aluminium (Canada). The aluminium frame can to a certain extent be adjusted and thereby adapted to individual experimental designs (e.g. adjustments of sample size). Figure 3.3 illustrates the aluminium frame (length/height/width 930/600/580mm) with two rails and a camera cradle on each rail.

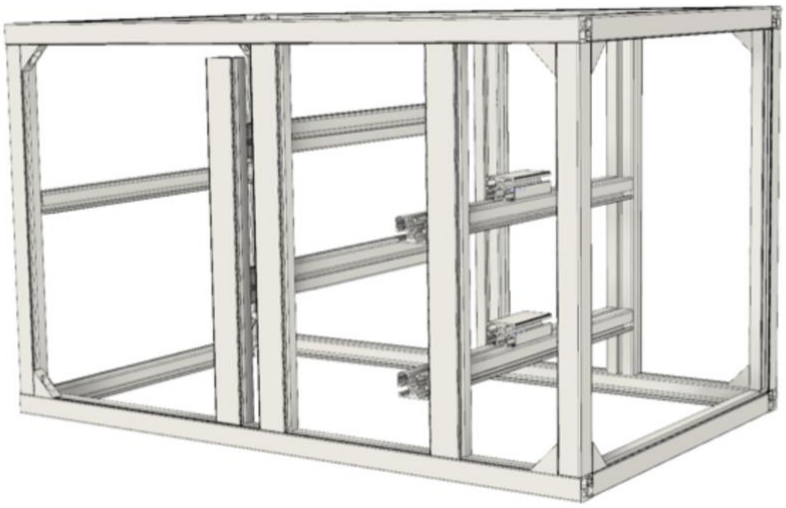

Figure 3.3. The figure illustrates the aluminium frame (length/height/width 930/600/580mm)

3.4 Soil cuvettes and artificial roots

Figure 3.4 illustrates the cuvettes (height/width/depth: 55/50/5 mm) made in Fusion 360 developed by Autodesk Inc. The cuvettes were 3D printed in Polylactic acid (PLA) plastic manufactured by Add North AB on a Ultimaker 3+ manufactured by Ultimaker B.V. Screws were attached on the back of these cuvettes so that they can easily be attached and fixed in position in the platform. The cuvettes have two inlets-outlets (~ 1.2mm x 2cm) to enable rewetting of the soils. Semi-permeable cellulose membranes (dialysis tubing cellulose membrane, Merck KGaA, Germany) were used as root-analogues. The membranes are placed in the groove that goes across the cuvettes. The membranes have a diameter of 6 mm and the length of the roots was determined to 2.5 cm.

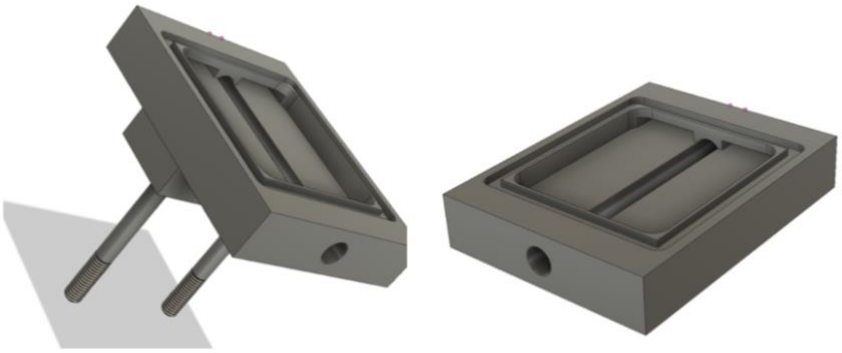

Figure 3.4. The figures illustrate the cuvette (height/width/depth: 55/50/5 mm): shown in profile, showing the screws attached on the backside (left) and shown oblique from above (right)

3.5 Drying system: PEG-solutions and pumps

The drying system consists of polyethylene glycol (PEG) 20'000 (Polyethylene glycol 20,000 (stabilized) for synthesis, Merck KGaA, Darmstadt, Germany) and peristaltic pumps (DULCO® flex DF2a Series, ProMinent, Heidelberg, Germany). The PEG substrate enables to obtain solutions with a certain osmotic potential. The osmotic potential of different concentrations [g 100 ml^{-1}] of the PEG-solution were measured using an Osmometer (Advanced® 3250 Single-Sample Osmometer, Molek, Sweden). This device uses freezing point-determination to measure the osmotic potentials of the solutions. Following Money (1989), the given osmotic potentials values in [mOsm/kg] were then converted into osmotic potentials values in [MPa]:

$$[MPa] = \frac{\left[\frac{\text{mOsm}}{\text{kg}}\right]}{1000}\ x\ 2.446$$

Graph 3.1 shows the calibration curve of osmotic potentials, illustrating how different concentrations of the PEG-solution imply different osmotic potentials.

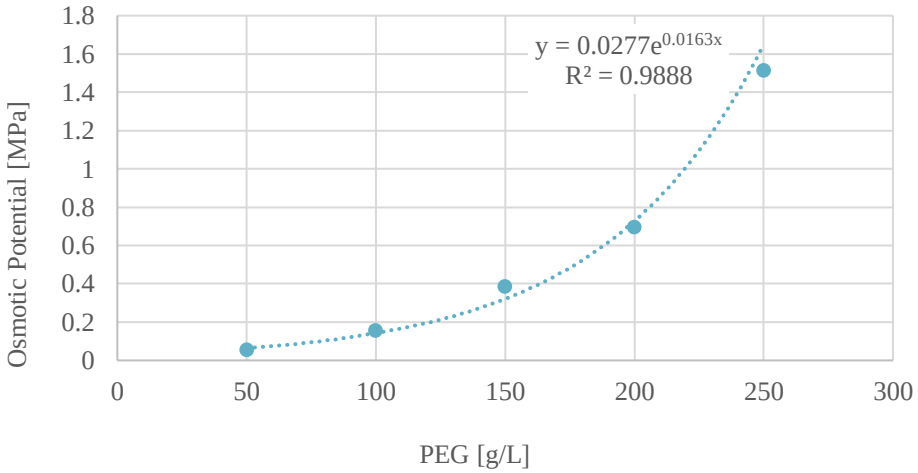

Graph 3.1. Calibration curve of osmotic potential, illustrating how different concentrations of the PEG-solution imply different osmotic potentials

3.6 Time-lapse imaging system

Two digital mirrorless interchangeable-lens cameras were used: Canon EOS M6 with Macro Lens EF-M28mm f/3 IS STM with Lens Hood ES-22 (Canon, Tokyo, Japan). The setting of the camera was: ISO100, Shutter 1/6, Aperture f22.

The two cameras were placed in camera holders in the aluminium frame. The camera holders are 3D printed in PLA plastic manufactured by Add North AB on a Ultimaker 3+ manufactured by Ultimaker B.V. and fixed to the profiles with M4 screws. PLA 3D printed hoods were attached to the camera lenses, providing a constant LED light for every picture using a standard 8 mm wide 12V LED strip. Figure 3.5 illustrates the camera hood (left) and the dimensions of the camera hood (middle and right).

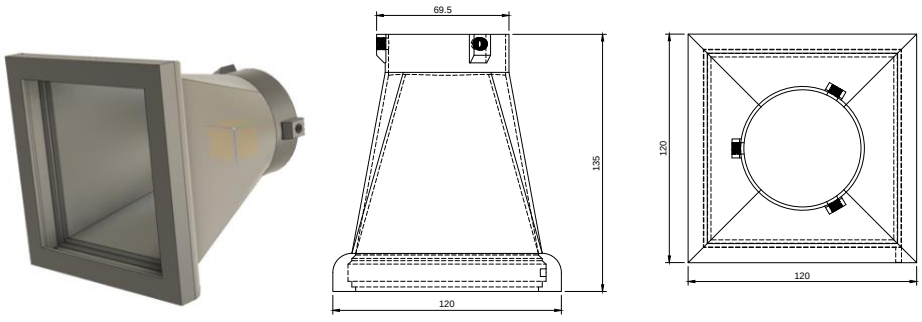

Figure 3.5. The figure illustrates the camera hood: picture of the camera hood (left) and sketches with the dimensions of the camera hood (middle and right)

The sleds are controlled by a bipolar NEMA17 1.8° 200 steps stepper motor manufactured by Luxorparts and standard GT2 belts and two GT2 Pulley Wheels for 3D printers. The movement of the camera was operated by an Arduino Mega 2560 from Arduino AG together with an Adafruit Motor Shield V2 (manufactured by Adafruit Industries, New York City, USA). In order to achieve time laps of exactly 2 minutes between each picture, an Arduino Micro has been added to give the Arduino Mega 2560 a signal every two minutes, upon which a loop is started.

The imaging is also controlled by the Arduino Mage 2560 and a 4N35 optocoupler manufactured by Vishay Intertechnology Inc (Malvern, Pennsylvania, USA). The system is programmed to capture one image every second minute of each cuvette. The programing for the Arduino cards have been made in Arduino IDE. The Arduino software consists of two stages: (1) the setup sequence and (2) the main loop. In the setup sequence the cradle travels to its starting position, i.e. homing sequence (switch). The setup sequence is followed by the main loop that starts after a two minutes' signal from the Arduino Micro card. The main loop consists of six photo shots. The shots are triggered by a pulse of 3.3V, sent from the Arduino Mega 2560 through the optocoupler to the camera via a modified standard remote cable soldered onto the PCB card. The camera moves between six different cuvettes before it returns to its starting position. The total camera travel length is 350 mm. When back at the starting position, the cradle is idle until the Arduino Micro sends the starting signal for the loop to start over again.

3.7 Image analysis

The obtained images will result in a series of images over the period of seven days for each treatment. We analyse the temporal development of cracks. The quantitative assessment of emerging cracks focused on the number of cracks, crack width and crack length. For analyses of the drying of the soil, treatment means of moisture changes were computed and plotted using the statistical software R version 3.3.3.

4 Experimental case study

4.1 Soil sampling, soil characteristics and root water potentials

The two soils used in this study were collected in the Uppsala region in Sweden: Säby and Ultuna. Table 4.1 summarizes the soil characteristics. The selection of the soils was based on differences in clay content, and thus differences in mechanical properties, i.e. differences in shrink and swell behaviour. To obtain homogenized soils and remove larger particles (>2mm) and plant litter, the samples were sieved through a 2mm mesh. The soils were also subjected to textural analysis by using the pipette method. The textural composition was for the Säby soil 21.5% clay, 52.8% silt, 25.8% sand, and for the Ultuna soil 42.1% clay. 31.4% silt, and 26.5% sand, classified as Loam and Clay respectively.

The gravimetric water contents, *w*, of the sieved soils were computed by weighing before and after oven drying for at least 24 hours at 105 °C. The particle density (ρ_s) was computed from the volume displacement of the soils in a glass flask with ethanol and the weight of the oven dried (105°C) soils. The bulk density (ρ_{bulk}) was set to 1.3 g cm^{-3}. This level was determined based on prior tests and was suitable to use for the two different soil types. Typical values are in the range 1.1-1.7 g cm^{-3} (Young et al. 1991, Young 1998). The total porosity (ε) was computed from the value of the bulk density and the particle density.

The amount of soil organic matter (SOM) was determined by combustion. SOM was approximated from the loss on ignition with a reduction factor related to the clay content. To obtain the loss of ignition the soils were first oven-dried over night at 105°C to remove water. After that, the soils were oven-dried at 550°C for 4 hours to obtain the loss of ignition. The soils

were stored in a fridge at 4°C and thoroughly wrapped in plastic to avoid water loss. The SOM content was 3.5% for Säby, and 0.6% for Ultuna.

Table 4.1. Soil characteristics including textural composition, SOM, gravimetric water content, bulk density, particle density and total porosity of the soils

Soil	Clay (%)	Silt (%)	Sand (%)	SOM (%)	Gravimetric water content (gg^{-})	Particle density (gcm^{-3})	Bulk density (gcm^{-3})	Total porosity (m^3m^{-3})
Säby	21.5	52.8	25.8	3.5	0.38	2.56	1.3	0.49
Ultuna	42.1	31.4	26.5	0.6	0.39	2.65	1.3	0.51

Two root water potentials were simulated in this experiment. To simulate the different root water potentials, two different osmotic potentials were used. The different osmotic potentials were obtained by using different concentrations of the PEG-solution. The selected values were: (A) -350 kPa; (B) -1500 kPa. These levels correspond to values used for simulation in related research (Delage & Cui 2008).

4.2 Sample preparation

Figure 4.1 describes the preparation procedure in 10 steps. The membranes were soaked in deionized water before usage. After that, they were attached, in each end, to silicon tubes (with inner diameter 4mm) using couplers and thereafter inserted into the cuvettes. The roots were placed in the grooves in the centre of the cuvettes. The cuvettes were filled with so much sieved soil that it obtained a bulk density of 1.3 g/cm^3. Thereafter was water added to reach 80% of the gravimetric water content at saturation.

The soils were then spread and equalized to obtain a smooth surface. Rubber bands were placed in the grooves around the soils on the cuvettes. A transparent glass-plate (6.5 x 8.5 x 2 mm) was placed on top of the front side of the cuvettes. Before placing the glass-plate, it was moistened with anti-fog drops (Look clear, S.R.L., Lecco, Italy). Drops were added and spread out and let acting before rinsed with deionized water. This solution is of importance to avoid fog appearance.

Thereafter, the cuvettes were hermetically sealed with parafilm (Parafilm® M laboratory film, Bemis Company Inc, USA). This in order to fix the glass-plates and to prevent water loss. The two outlets from the tubes were closed using couplers. The prepared cuvettes were left resting for two days to ensure homogenous water distribution. The PEG-solutions were prepared by adding PEG to deionized water in the required concentrations.

The prepared cuvettes were then fixed and positioned in the two rows closest to the pumps, 6 cuvettes on each row. It cannot be any fog on the glass-plates during the experiment and the parafilm should not cover the soil area. If fog has occurred, corrections are motivated. The pumps were connected via tubes to the cuvettes and the PEG-solution reservoirs that were placed on the roof of the platform, above the cuvettes and close to the pumps. The camera hoods were attached to the cameras. This is done to obtain a constant light and avoid reflectance. During the experiment the platform was darkened to assure constant light conditions.

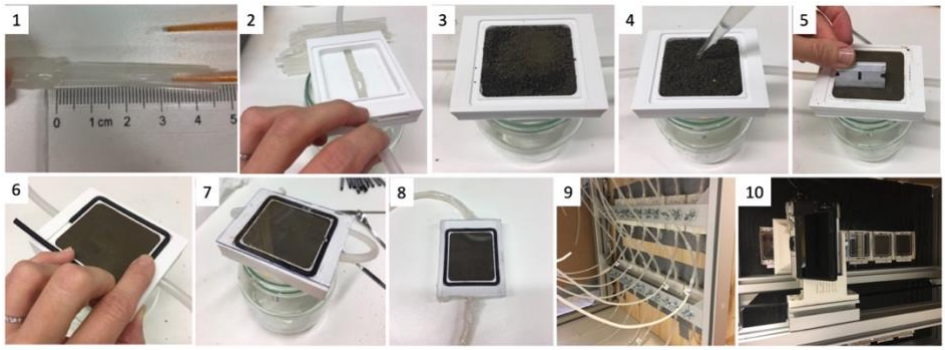

Figure 4.1. The preparation procedure in 10 steps: (1) the construction of the root (2) root inserted into the cuvette (3) soil-filling in the cuvette (4) water added to the soil (5)the soil is spread and equalized to obtain a smooth surface (6) the placement of the rubberband around the soil on the cuvette (7) the placement of the glass-plate (8) the cuvette sealed with parafilm (9) the cuvettes placed in the framework showing the backside where they are attached with screws (10) camera hood attached to the camera that are placed in the camera holder facing the cuvettes with surrounding black wall

4.3 Computing changes in moisture

After the image scanning, the cuvettes were removed. Some sample data were excluded because of leakage from the tubes during the experiment. The outlets of each cuvette were sealed to prevent further water losses. Figure 4.2 illustrates how the soils in the cuvettes were split into 20 equal evenly distributed pieces (~ 1.25 x 1.1mm). This was done with a razorblade. All pieces were then weighed.

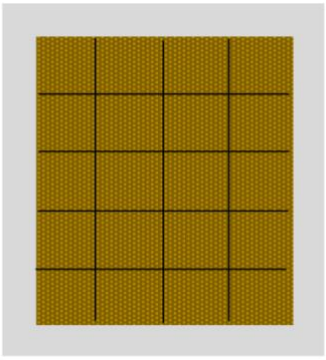

Figure 4.2. Illustration of the distributed pieces that were weighted before and after drying to generate the gravimetric water content

After that, all pieces were dried in an oven at 105 °C for 24 h and then weighed again. This resulted in information on the gravimetric water content before and after the experiment, which were then used to generate the spatial distribution of the change in moisture, i.e. drying of the soils.

First, average soil moisture was computed as the mean of the different replicates. We then calculated the water loss. After that, we interpolated the change in the moisture of the soils, which corresponds to how the soils have dried. The mean moisture change [g g^{-1}] was then plotted. These figures show how the soils have dried spatially around the roots due to water uptake.

5 Results

The experiment provided images every second minute over a period of 7 days. For each unit sample, 5 760 images were recorded. In total, 138 240 images have been collected from the time-lapse imaging. In this experimental case study, eight units out of 12 were used in each round, resulting in 16 sample units.

5.1 Crack formation

Figures 5.1 to 5.4 show image series of the crack formation for each treatment from the start of the experiment (0) until the end of the experiment, i.e. after seven days (7d). Cracks developed fast and emerged within the first day. The cracks first develop horizontally around the roots and then vertically along the roots. Neither the number of cracks nor crack patterns change that much in the following days. Nevertheless, both the length and width of the cracks somewhat extends, the cracks elongate and enlarge over time. This is true for all treatments levels.

The clay rich Ultuna soil appears to induce higher numbers of cracks that also are longer and wider (Figures 5.1 and 5.2) than those in the Säby soil (Figures 5.3 and 5.4). The Säby soil, which consists less clay, behaves differently. The cracks are much smaller and less extensive in their spatial formation. Same trends are observed whilst comparing the different root water potentials. As the soils are exposed to a lower root water potential, higher numbers of cracks have emerged and the cracks are both wider and longer. This can be seen when comparing the Ultuna soil at root water potential -350 kPa (Figure 5.1) and at root water potential -1500kPa (Figure 5.2). This is also true comparing the Säby soil at root water potential -350 kPa (Figure 5.3) and at root water potential -1500kPa (Figure 5.4).

In a comparison between the different treatment levels, the combination of a clay rich soil and a lower root water potential induced more number of cracks and cracks that are longer and wider. This is illustrated in Figure 5.3 showing the Ultuna soil with a root water potential of -1500 kPa, which is in contrast to the Säby soil with root water potential -350 kPa as shown in Figure 5.2. From the perspective of morphology of the crack network, we can see that the soils crack horizontally along with the location of the roots and vertically out from the roots. Cracks are also emerging along with the borders of the cuvettes as the soils gradually shrink from the boarders of the cuvettes.

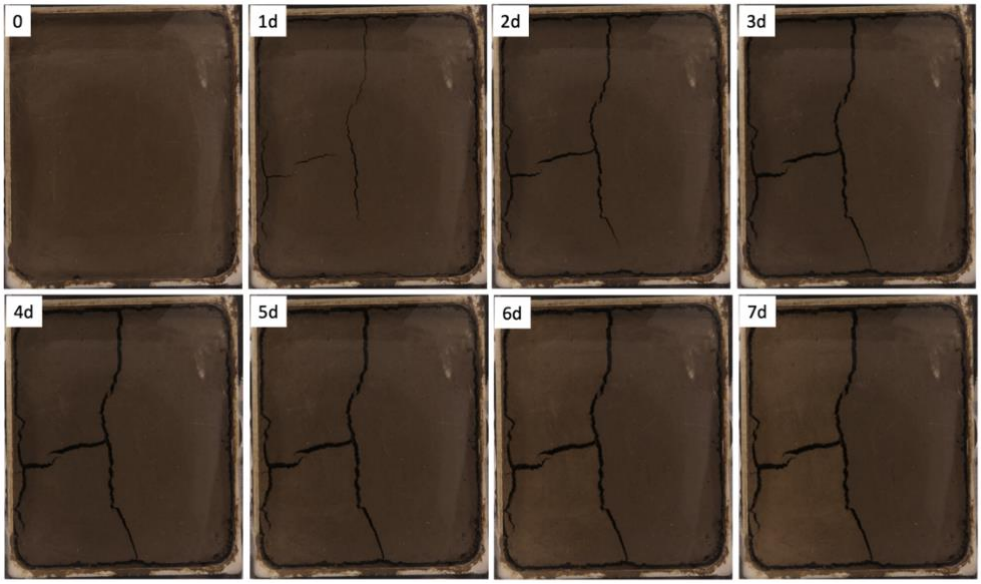

Figure 5.1. Crack formation over the period of 7 days in the Ultuna soil with the root water potential -350 kPa

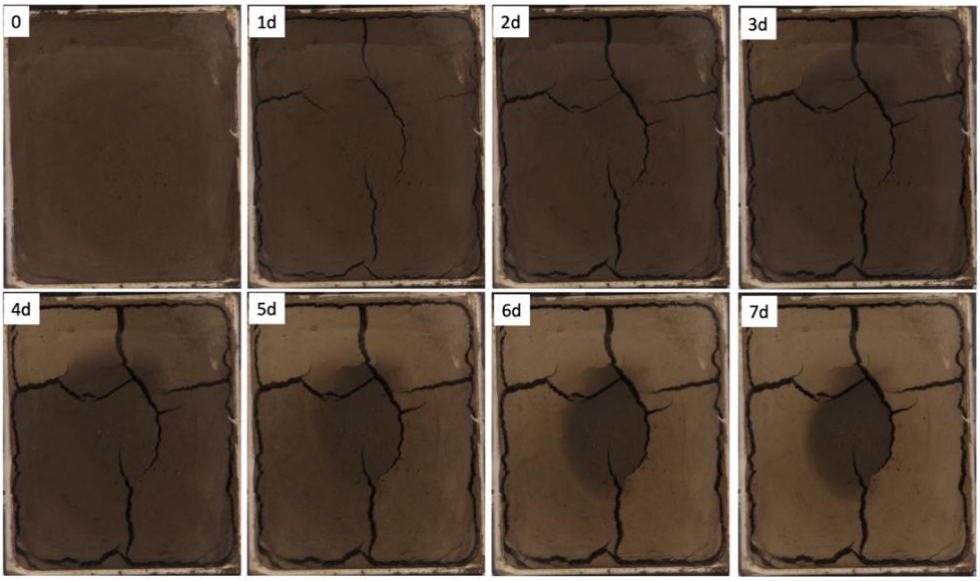

Figure 5.2. Crack formation over the period of 7 days in the Ultuna soil with the root water potential -1500 kPa

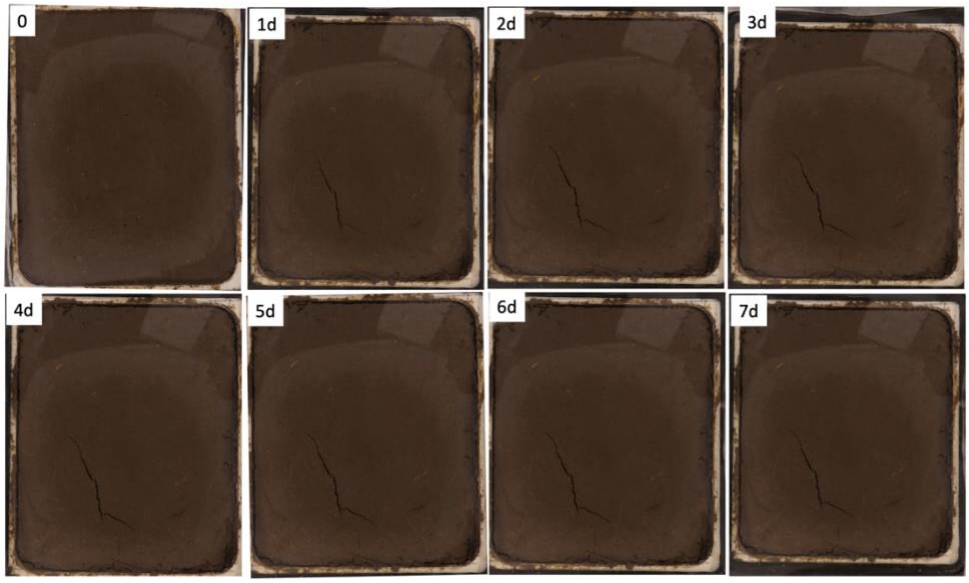

Figure 5.3. Crack formation over the period of 7 days in the Säby soil with the root water potential -350 kPa

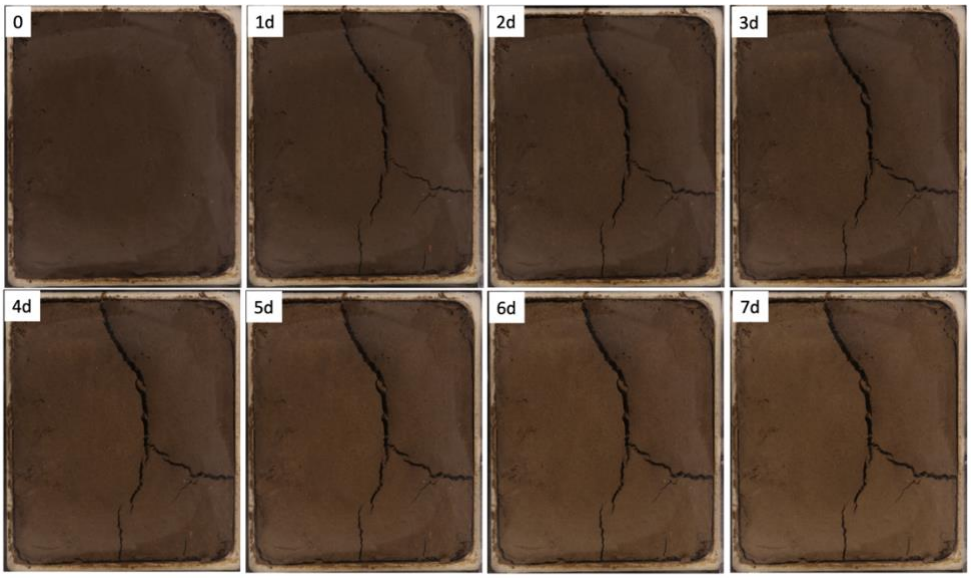

Figure 5.4. Crack formation over the period of 7 days in the Säby soil with the root water potential -1500 kPa

5.2 Colour changes

Colour changes in the images indicate drying of the soils. The drying patterns differ amongst the treatments, depending on both the soil type and the root water potential. As we can see, the Ultuna soil (Figures 5.1 and 5.2) has a more uneven drying pattern in comparison to the Säby soil that has dried more evenly across the cuvettes (Figures 5.3 and 5.4). The Ultuna soil with the root water potential -350 kPa (Figure 5.1) shows little, if any at all, changes in colour the first four days. Thereafter, colour changes can be observed, and the changes are greater to the left of the root.

The Ultuna soil with the root water potential -1500 kPa (Figure 5.2) shows the first two days a change in colour evenly distributed, but thereafter, from the third day, it seems like the pattern is more uneven. The drying gradually becomes higher around the borders of the cuvettes over time, and in the end the colour indicates very dry soil, except close to the root. The colour becomes gradually brighter in the Säby soil over time, and it visually seems that the change in colour is evenly distributed, both at root water potential -350 kPa (Figure 5.3) and at root water potential -1500 kPa (Figure 5.4).

At the end of the experiment, it appears that the colour changes, are greatest in the Ultuna soil with the root water potential -1500 kPa (Figure 5.2), although the soil near the root is still wet. Also, the Säby soil with the root water potential -1500 kPa (Figure 5.4) shows substantial colour changes. These changes appear evenly distributed across space. Overall, a clay rich soil implies uneven drying patterns (Figure 5.1 and 5.2) and a lower root water potential dries the soil to a greater extent (Figure 5.2 and 5.4).

5.3 Drying of the soils

Figures 5.5 and 5.6 show the change [g g^{-1}] in moisture, i.e. drying, of the soils at the end of the experiment. The higher value (closest to zero) indicates a relatively small change in moisture towards drying, and vice versa. Note that the scale values vary in the legends across the figures.

The clay rich Ultuna soil with the root water potential -1500 kPa induce the highest mean moisture change, -0.201 gg^{-1}, while at -350 kPa, the change was -0.133 gg^{-1}. Minimum and maximum moisture change was for the Ultuna soil from -0.118 to -0.126 gg^{-1} with a root water potential of -350 kPa and from -0.18 to -0.23 gg^{-1} with a root water potential of -1500 kPa. (Figure 5.5). The lowest mean moisture change was found in the Säby soil with the root water potential -350 kPa that dried -0.101 gg^{-1}. However, the change was -0.193 gg^{-1} at --1500 kPa. Minimum and maximum moisture

change was for the Säby soil from -0.080 to -0.110 gg^{-1} with a root water potential of -350 kPa and from -0.18 to -0.225 gg^{-1} with a root water potential of -1500 kPa (Figure 5.6).

In all treatments, except for the Säby soil with the root water potential -350 kPa, we can observe a similar spatial distribution of the drying of the soils. The change in moisture was relatively lower around the roots and the drying gradually increased towards the edges. The Säby soil with the root water potential -350 kPa (Figure 5.6) showed a rather different spatial distribution in the change in moisture. The least and largest drying have taken place close to the edge but on opposite sides.

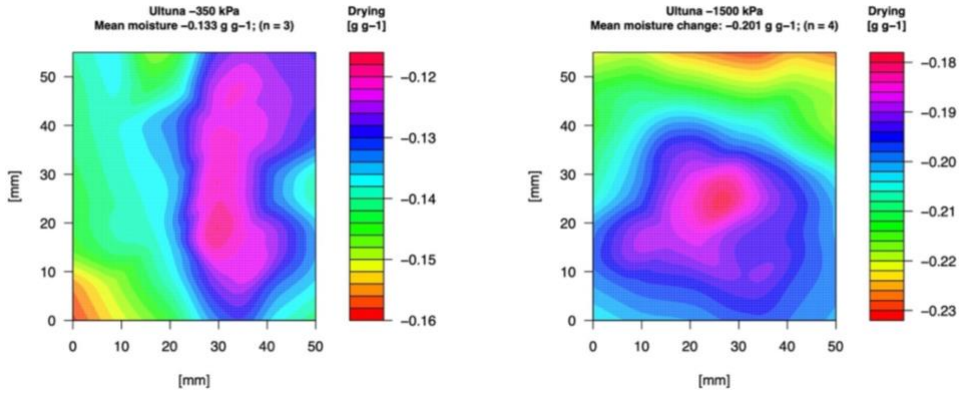

Figure 5.5. The spatial moisture change, i.e. drying, distribution in the Ultuna soil with the root water potential -350 kPa (left) and -1500 kPa (right)

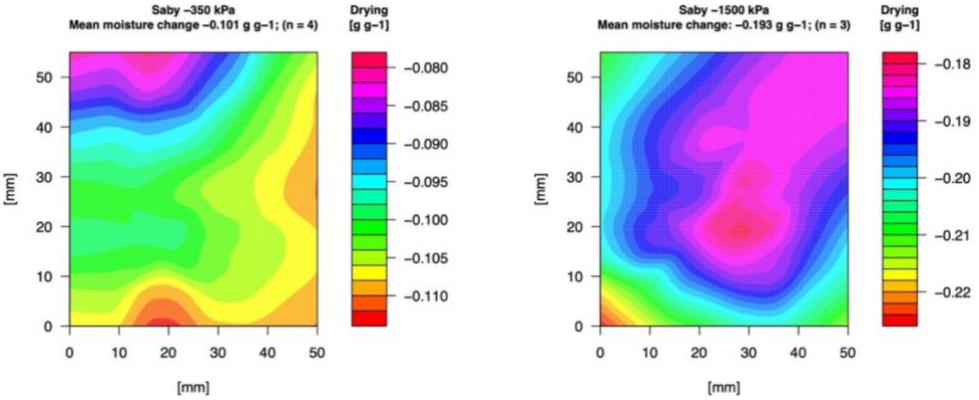

Figure 5.6. The spatial moisture change, i.e. drying, distribution in the Säby soil with the root water potential -350 kPa (left) and -1500 kPa (right)

6 Discussion

There were two main results from this study. The first concerns the validity of the employed method and the second concern the experimental results from the case study. Some future steps are also suggested.

6.1 Methodological considerations

The employed method is a novel and useful approach to study non-destructive and continuous spatiotemporal information of crack formation. One of the main advantages is that it provides a large quantity and very detailed information. It also enables tracking temporal changes in the soil. Overall, the experimental case study demonstrates that the employed method is both useful and acceptable to study crack formation due to plant water uptake. The approach has the capacity to provide images with a quality to make both visual assessments of crack formation and quantification of the spatial configuration of emerging cracks. The technical structure was relatively easy to set up and straightforward to implement. The process is automatized and non–destructive over a relatively long time period, in this study for 7 days. However, there are some issues to be considered before and during implementation of an experiment based on this approach. For instance, the artificial roots are sensitive, suggesting that root engineering is central to a successful experiment. It should be stressed to use appropriate and high quality technical components in the set-up, such as the pumps. The pumps must be durable and have enough capacity to make the PEG-solution flow continuously throughout the system. During the experiment for this study, several pumps broke down and had to be replaced, which delayed the extraction of results. There is also a risk for leakages in the system where the tubes are connected. Leakages may cause loss of the PEG-solutions and disturbances in the drying of the soils. There are also some engineering aspects that should be considered. For example, the framework of the platform must enable an appropriate placing of the

camera as reflections in the images of the soils may arise, which may influence the quality of the resulting images. Dark covering of the platform and efficient camera hoods are important to hinder quality reductions in the images.

6.2 Experimental results

The results presented in this study show that soil type and root water potential impact drying of the soils and crack development in different ways. The clay rich Ultuna soil (Figures 5.1 and 5.2) induced higher number of cracks, wider and longer cracks than those in the Säby soil (Figures 5.3 and 5.4), which had a lower clay content. A soil with greater clay content implies increased shrinkage and thus relatively higher number of cracks number, that are also wider and longer, and vice-versa, which confirms the hypothesis that clay controls the expansive properties of the soil (Oades 1993).

Furthermore, a relatively low root water potential (Figures 5.2 and 5.4) induced larger cracks in terms of numbers but also width and length than those with the higher root water potential (Figures 5.1 and 5.3). Amongst all treatments, the Ultuna soil with the lower level of root water potential had dried the most at the end of the experiment. As explained by Vereecken et al. (2016), this is expected as the suction of the roots influences the water uptake. However, the change in soil water content upon drying may alter the hydraulic conductivity and should thus influence the distribution of the drying. The hydraulic conductivity also differs depending on the textural composition of a soil. A clay soil has lower hydraulic conductivity in comparison to a sandy soil (Daly et al. 2018), which may explain the different drying patterns between the two soils (Figures 5.1 to 5.4). The fact that the change in moisture was relatively lower around the roots and the drying gradually increased towards the edges was unexpected. Reasons for this could be the size of the cuvettes that resulted in drying of the whole soil sample. However, at the end of the experiment it had not yet completely dried around the roots.

6.3 Next step and some suggestions on future work

This study shows that the employed method can be utilized to generate detailed information on soil dynamic features and processes. Hence, future applications are motivated. A new experiment based on the employed method is currently under development. One of the novel aspects of this

work will be the development and use of a new automatic protocol to generate quantitative data on the spatial configuration of emerging cracks. These data will enable very detailed analyses of crack development and how features such as crack areas, connectivity, length, width and number of cracks changes and develops over time. In turn, this may enable modelling and make predictions of the spatial impact of plant water uptake on crack formation.

Future research is suggested to consider the use of living roots in experiments. The roots of living plants would respond to the changes in soil properties that arise due to drying in a way that was not possible for the artificial roots. This could also contribute to improve soil-root interaction models. Living roots could also be used to analyze how different crops and/or varieties impact crack formation. Another suggestion is to increase the size of the cuvettes. This is motivated as cracks were observed to emerge towards the edges and around the borders of the cuvettes. With increased sample sizes, we would be able to assess the full impact of root water uptake on crack development. Rewetting of the soils is another interesting aspect that could be analyzed, as the effect of several wetting and drying cycles may alter the crack features and the development of cracks.

7 Conclusions

This study makes two main contributions. First, it proposes a novel experimental method that enables analysis of crack formation and drying of the soil around artificial roots due to root water uptake at high spatial (10 µm) and temporal (2 min) resolution. The employed method provides images every second minute over a time period of 7 days. The experiment resulted in images with a sufficient quality to make visual assessments of crack formation and quantification of the spatial configuration of emerging cracks. Second, the study shows that plant water uptake affects crack formation and drying of the soils differently. This depending on soil type and root water potential. Soils with higher clay content and/or a higher root water potential induce more cracks and cracks that are relatively longer and wider. The analysis of the spatial distribution of drying of the soil suggests more drying of the soil around roots with higher clay content and with lower level of root water potential. This is expected as clay contains expansive properties of the soil and a lower root water potential dries the soil to a greater extent. The results are consistent with related theory and prior studies. Overall, the results demonstrate that the employed experimental method is both useful and valid to study crack formation due to plant water uptake.

Acknowledgements

I wish to thank my main supervisor Dr Tino Colombi for encouragement, excellent feedback and guidance throughout this work. I am also grateful to my assistant supervisor Professor Thomas Keller who has also been very supportive and provided excellent feedback and constructive suggestions. I would also like to thank Research Engineer Daniel Iseskog for technical support and Laboratory Engineer Ana Mingot for analysis of the soils. Naturally, I also wish to thank everyone at the Department of Soil and Environment at the Swedish University of Agricultural Sciences (SLU) in Uppsala. The thesis was made within the research project "ImproSoSt" (Marie Skłodowska-Curie Actions, Call identifier: H2020-MSCA-IF-2017 H2020-MSCA-IF-2017).

References

Angers, D., & Caron, J. (1998) Plant-induced Changes in Soil Structure: Processes and Feedbacks. Biogeochemistry 42(1): 55-72. doi:10.1023/A:1005944025343

Ball, R.A., Oosterhuis, D.M. (2005) Measurement of root and leaf osmotic potential using the vapor-pressure osmometer. Environmental and Experimental Botany 53: 77–84

Bronick, C.J., Lal, R. (2005) Soil structure and management: a review. Geoderma 124 (1): 3-22. doi:10.1016/j.geoderma. 2004.03.005

Bodner, G., Scholl, P., Kaul, H.P. (2013) Field quantification of wetting–drying cycles to predict temporal changes of soil pore size distribution. Soil Tillage Research 133: 1–9

Carminati, A., Moradi. A., Vetterlein, D., Vontobel, P., Lehmann, E., Weller, U., Vogel. HJ., Oswald. S. (2010) Dynamics of soil water content in the rhizosphere. Plant and Soil 332(1): 163–176. doi: 10.1007/s11104-010-0283-8

Carminati, A., M. Zarebanadkouki, M., Kroener, E., Ahmed, M. A., Holz, M. (2016) Biophysical rhizosphere processes affecting root water uptake, Annals of Botany 118(4): 561-571. https://doi.org/10.1093/aob/mcw113

Daly, K., Tracy, S., Crout, N., Mairhofer, S., Pridmore, T., Mooney, S., & Roose, T. (2018) Quantification of root water uptake in soil using X-ray computed tomography and image-based modelling. Plant, Cell & Environment 41(1): 121-133

DeCarlo, K.F, & Shokri, N. (2014) Effects of substrate on cracking patterns and dynamics in desiccating clay layers. Water Resources Research 50(4):3039-3051. doi: 10.1002/2013WR014466

Delage, P., Cui, Y.J. (2008) An evaluation of the osmotic method of controlling suction, Geomechanics and Geoengineering: An International Journal 3(1): 1-11, doi: 10.1080/17486020701868379

Dexter, A.R (1991) Amelioration of soil by natural processes. Soil and Tillage Research 20(1): 87-100. doi: 10.1016/0167-1987(91)90127-J

Elkins, N., Sabol, Z., Ward, G., & Whitford, W. (1986) The influence of subterranean termites on the hydrological characteristics of a Chihuahuan desert ecosystem. Oecologia 68(4): 521-528. doi: 10.1007/BF00378766
Eriksson, J., Dahlin, S., Nilsson, I., Simonsson, M. (2011) Marklära. Studentlitteratur
Garrigues, E., Doussan, C., & Pierret, A. (2006) Water Uptake by Plant Roots: I – Formation and Propagation of a Water Extraction Front in Mature Root Systems as Evidenced by 2D Light Transmission Imaging. Plant and Soil 283(1): 83-98. doi: 10.1007/s11104-004-7903-0
Guimarães, RML., Lamandé, M., Munkholm, LJ., Ball, BC., & Keller, T. (2017) Opportunities and future directions for visual soil evaluation methods in soil structure research. Soil & Tillage Research 173: 104-113. doi: 10.1016/j.still.2017.01.016
Helliwell, J., Sturrock, C., Mairhofer, S., Craigon, J., Ashton, R., Miller, A., Whalley, W.....Mooney, S. (2017) The emergent rhizosphere: Imaging the development of the porous architecture at the root-soil interface. Sci Rep 7. Article number: 14875. doi: 10.1038/s41598-017-14904-w
Jangorzo, N., Watteau, S., Hajos, F., & Schwartz, D. (2015) Nondestructive monitoring of the effect of biological activity on the pedogenesis of a Technosol. Journal of Soils and Sediments 15(8): 1705-1715
Jin. K., White P.J., Whalley. WL., Shen. J., Shi. L. (2017) Shaping an Optimal Soil by Root–Soil Interaction. Trends in Plant Science 22(10): 823-829. doi: 10.1016/j.tplants.2017.07.008
Johannes, A. (2016) Structural Degradation of Agricultural Soils: Assessment and Setting Threshold Values for Regulation. Doctoral dissertation. ETH Zurich: https://www.research-collection.ethz.ch/handle/20.500.11850/47
Kay B.D. (1998) Soil structure and organic carbon: A review. In: Lal, R., et al., Ed., Soil Processes and the Carbon Cycle, CRC Press, Boca Raton: 169-197
Keller, T., Colombi, T., Ruiz, S., Pogs Manalili, M., Rek, J., Stadelmann V., Wunderli, H., Breitenstein, D., Reiserer, R., Oberholzer, H., Schymanski S., Romero-Ruiz, A., Linde, N., Peter Weisskopf, P., Walter, A and Or, D. (2017) Long-Term Soil Structure Observatory for Monitoring Post-Compaction Evolution of Soil Structure 16(5) https://doi.org/10.2136/vzj2016.11.0118
Lavelle, P. (1997) Faunal Activities and Soil Processes: Adaptive Strategies That Determine Ecosystem Function. Advances in Ecological Research 27(C): 93-132. doi: 10.1016/S0065-2504(08)60007-0
Money, N.P. (1989) Osmotic pressure of aqueous polyethylene glycols. relationship between molecular weight and vapor pressure deficit. Plant Physiology (2): 766-769

Oades, J.M. (1993) The role of biology in the formation, stabilization and degradation of soil structure. Geoderma 56(1): 377-400. doi: 10.1016/0016-7061(93)90123-3
Rabot. E. Wiesmeier. M.Schlüter. S. Vogel. H.-J. (2018) Soil structure as an indicator of soil functions: A review. Geoderma 314: 122-137. doi: 10.1016/j.geoderma.2017.11.009
Six J., Bossuyt H., Degryze S., Denef K. (2004) A history of research on the link between (micro) aggregates, soil biota, and soil organic matter dynamics. Soil and Tillage Research 79(1): 7-31. doi: 10.1016/j.still.2004.03.008
Starkloff, T., Larsbo M., Stolte, J., Hessel R., Ritsema C. (2017) Quantifying the impact of a succession of freezing-thawing cycles on the pore network of a silty clay loam and a loamy sand topsoil using X-ray tomography. Catena 156: 365–374. doi: 10.1016/j.catena.2017.04.026
Taina, I.A., Heck, R.J., Elliot, T.R. (2008) Application of X-ray computed tomography to soil science: a literature review. Can. J. Soil Sci. 88 (1): 1–19
Tang, C-S,. Wang, D-Y., Zhu, C., Zhou, Q-Y., Xu, S-K., & Shi, B. (2018) Characterizing drying-induced clayey soil desiccation cracking process using electrical resistivity method. Applied Clay Science 152: 101-112. doi: 10.1016/j.clay.2017.11.001
Tisdall, J.M., Smith, S.E., Rengasamy, P. (1997) Aggregation of soil by fungal hyphae. Australian Journal of Soil Research 35(1): 55–60
Tracy, S., Black, C., Roberts, J., Sturrock, C., Mairhofer, S., Craigon, J., & Mooney, S. (2012) Quantifying the impact of soil compaction on root system architecture in tomato () by X-ray micro-computed tomography. Annals of Botany 110(2): 511-519
Vereecken, H, Schnepf, A, Hopmans, Jw, Javaux, M, Or, D, Roose, T, . . . Young, I.M. (2016) Modeling soil processes: Review, key challenges, and new perspectives. Vadose Zone Journal 15(5): 1-57. doi: 10.2136/vzj2015.09.0131
York, L., Carminati, A., Mooney, S., Ritz, K., & Bennett, M. (2016) The holistic rhizosphere: Integrating zones, processes, and semantics in the soil influenced by roots. Journal Of Experimental Botany 67(12): 3629-3643
Young, I.M., Mullins, C.E., Costigan, P.A., Bengough, A.G. (1991) Hardsetting and structural regeneration in two unstable British sandy loams and their influence on crop growth. Soil and Tillage Research 19(4): 383–394. doi: 10.1016/0167-1987(91)90114-D
Young, I., Blanchart. E., Chenu, C., Dangerfield. M., Fragosos, C., Grimaldi. M., Ingram. J., Monrozier, L.J. (1998) The interaction of soil biota and soil structure under global change. Global Change Biology 4(7): 703–712. doi: 10.1046/j.1365-2486.1998.00194.x

Young, I.M (1998) Biophysical interactions at the root–soil interface- a review. Journal of Agricultural Science, Cambridge 130(1): 1–7
Wang, S., Yang, P., Yang, Z. (2018) Characterization of freeze–thaw effects within clay by 3D X-ray Computed Tomography. Cold Regions Science and Technology 148: 13–21.
doi: 10.1016/j.coldregions.2018.01.001
Zhang, W., T.H. Ricketts, C. Kremen, K. Carney, and S.M. Swinton. (2007) Ecosystem services and dis-services to agriculture. Ecol. Econ. 64:253–260. doi:10.1016/j.ecolecon.2007.02.024